CIRCULATION IN THE OUTER NEARSHORE ZONE

H. Tuba Özkan-Haller[1]

Abstract

We further explore the dynamics of currents just outside the surf zone, where circulation appears to result from a delicate balance between several weak forcing mechanisms, including wave forcing, effects of Earth's rotation through the Stokes-Coriolis surface stress and the Coriolis terms in the momentum equations. Also important are turbulent mixing terms and surface and bottom boundary layer effects. We analyze the temporally varying response to a one-month time series of waves typical for the East Coast of the US. We find intriguing behavior in the time-dependent circulation including oscillations at inertial frequencies with amplitudes that can exceed the steady state response amplitudes.

Key words: hydrodynamics, nearshore circulation, outer surf zone, Coriolis parameter, temporal variability in currents, canonical test case

1. Introduction

Surf zone longshore currents or rip currents are forced primarily by mechanisms related to wave breaking. Horizontal mixing processes or advective effects often lead to the extension of the influence of these currents to the deeper waters of the outer nearshore zone where other forcing mechanisms are also active. For example, wind-induced flows can be observed in these waters (Fewings et al., 2008), and both wind-driven and wave-driven transport may be at work simultaneously (Kirincich et al., 2005). Hence, the outer surf zone is an area where weak wave forcing and mixing effects are present, but weak wind and Coriolis-driven forcing mechanisms, often neglected in the surf zone, are also effective. As a result, the flows just outside of the surf zone may be the result of a delicate balance between several weak forcing mechanisms.

Herein, we are interested in examining flows just outside the surf zone, taking into account the multiple forcing mechanisms mentioned above. In particular, we will consider the effects of Earth's rotation (via the Coriolis term) on the wave-averaged circulation as well as its effect on the incident waves (explained further below). We are also accounting for surface and bottom boundary layer effects, including the effects of surface gravity waves in these boundary layers. Finally, we will account for the (albeit weak) surf zone forcing mechanisms related to radiation stress gradients and roller effects. The resulting model was analyzed for an idealized beach setting by Özkan-Haller (2013), and their results indicated that the circulation just outside the surf zone may be significantly affected by Coriolis effects. Here, we analyze this effect further and provide examples of possible circulation magnitudes for realistic wave forcing events.

2. Approach

We analyze the potential importance of physical processes in the outer nearshore zone by assembling a model of wave-averaged currents considering several forcing mechanisms. The relevant processes are

1. Forcing terms related to the radiation stress gradient and men setup terms. These result in a depth-independent body force F (Svendsen et al, 20xx).
2. Forcing terms related to the Coriolis-Stokes stress that results from the effect of the Earth's rotation on surface gravity waves (Hasselman, 1970; Xu and Bowen, 1994). Although the alongshore velocities generated by the effect of Earth's rotation on surface gravity waves are small, the resulting along-crest velocity component is nonetheless in phase with the vertical orbital velocity, resulting in a small but non-zero stress that is mostly active near the top of the water column.

[1]College of Earth, Ocean, and Atmospheric Sciences, Oregon State University, Corvallis, OR 97331, USA, ozkan@coas.oregonstate.edu.

3. Terms that are related to the effects of the Earth's rotation on the circulation with the use of a Coriolis term in the momentum equations
4. Surface boundary layer stress terms including the shoreward shear stress caused by the presence of wave breaking rollers
5. Bottom boundary layer effects, and
6. Effects of turbulent momentum mixing parameterized using an eddy viscosity formulation and include.

The resulting model equations are similar to those considered by Xu and Bowen (1994), but contain the surf zone body forcing term (item 1 above) that was also included by Lentz et al. (2008). Following Özkan-Haller (2013), we also include a surface stress term due to the presence of rollers, and an eddy viscosity formulation that includes a simple representation of the turbulence generated by wave breaking (Battjes, 1975). Note that the model assumes the presence of random irregular waves. The resulting equations for the horizontal momentum (in steady state form) are

$$\frac{\partial}{\partial z}\left\{\nu_t \frac{\partial U}{\partial z}\right\} + fV = F + \frac{\partial \langle \tilde{u}\tilde{w} \rangle}{\partial z} \tag{1}$$

$$\frac{\partial}{\partial z}\left\{\nu_t \frac{\partial V}{\partial z}\right\} - fU = \frac{\partial \langle \tilde{v}\tilde{w} \rangle}{\partial z} \tag{2}$$

where *U* and *V* are the horizontal velocities in the cross-shore and alongshore directions, respectively. The effects of Earth rotation are included in the second terms on the left hand sides of equations (1) and (2) (item 3 in the above list). The value of the Coriolis parameter *f* corresponds to mid-latitudes and is, therefore, O(10^{-5}). The forcing terms on the right hand side of equation (1) account for the surf zone body force *F* (item 1 above), and the non-zero shear stress generated at the bottom due to boundary layer effects (item 5 above). The orbital velocities associated with the surface gravity waves are indicated as $(\tilde{u}, \tilde{v}, \tilde{w})$, and the brackets $\langle\ \rangle$ indicate averaging over the wave time scales. Effects of turbulent momentum mixing are included using a simple eddy viscosity (ν_t) closure (item 6 above), which is assumed to be uniform over depth but is allowed to vary in the cross-shore direction according to Battjes (1975).

The Coriolis-Stokes stress (item 2 above) is represented in equation (2) as the last term and is non-zero because the along-crest orbital velocity component generated due to the effect of Earth's rotation on the gravity waves is in phase with the vertical orbital velocity (Hasselman, 1970). Note that the along-crest velocity component is very small ($O(f/\sigma) = 10^{-4}$, where σ is the angular frequency of the incident waves), the generated stress can nonetheless be O(0.1Pa) and hence similar in size to the wind stress on the inner shelf (Xu and Bowen, 1994). This stress is often neglected in circulation models of the inner shelf, yet has recently been shown to be a potentially important player in the dynamics of the inner shelf (Lentz et al., 2008) and all the way into the region just outside the surf zone (Özkan-Haller, 2013).

Finally, the surface shear stress due to the presence of rollers (item 4 in the above list) is imposed as a surface boundary condition, where the surface stress is

$$\tau_{rS} = \frac{\varepsilon_r}{c} \tag{3}$$

The remaining boundary conditions dictate no flow at the bottom boundary, and conservation of volume flux in the cross-shore direction, ensuring that the shoreward directed surface mass flux due to the gravity waves is returned offshore by the depth-integrated undertow flux. This last boundary condition determines the magnitude and cross-shore variation of the body force *F*. The shoreward mass flux due to the waves includes the contribution dictated by linear wave mechanics as well as the roller surface flux computed according to Svendsen (1984). The resulting formulation of the surface shear stress and volume flux is equivalent to the treatment of Newberger and Allan (2007).

The reader is referred to Özkan-Haller (2013) and the references therein for the complete set of governing equations as well as details on the analytical solution. Here, we only note that the assembled model equation is linear in the unknown horizontal velocity components so that the predicted current can be analyzed as the summation of current components that result as a consequence of the individual processes mentioned above. This analysis was carried out for a canonical case involving a barred beach by Özkan-Haller (2013), and the steady state solution indicates the presence of circulation features that are not predicted by traditional undertow models that don't take into the account the set of processes included here. Below we construct a canonical example case involving a plane beach and point out some of the features for the resulting circulation.

One additional consideration for the solution including Coriolis effect is the question regarding the time scale of the resulting response. In general, Coriolis-influenced circulation occurs at a time scale that is related to the Earth's rotation, hence O(1 day). Since wave conditions usually change over such time scales, the steady state solution may never be attained. In this paper, we analyze the resulting circulation in a time-varying setting using realistic wave time series over the course of a month. The time varying solution derived by Xu and Bowen (1994) is utilized.

3. Results

The canonical case utilized herein involves a plane beach with slope m=0.025. We consider an alongshore-uniform beach and place the offshore boundary 2km from shore in 50m water depth. At this offshore boundary waves of given wave height are introduced. We consider a simulation that covers a month. In particular, an hourly time series of waves at the National Data Buoy Center (NDBC) Onslow Bay buoy (#41036) on the Atlantic Coast of the USA during March 2013 is considered. To isolate the effect of wave height variability, we neglect wave period variations and consider a constant mean wave period of ~8sec. The wave height time series varies (see Figure 1) appreciably with wave height values of 1m increasing to 2-3.25m during multiple storms of multiple day durations. In order to gain a better understanding of the resulting circulation, we first analyze the steady state response to a wave field with wave height 1m, 2.25m, and 3.25m.

Next, we consider the possibility that the circulation cannot reach steady state before a significant change in the wave field occurs (e.g. passage of the storm). We first consider an idealized situation that consist of a series of wave events with constant wave height. These are chosen to roughly mimic the one-month time series from buoy 41036 (see Figure 1 for a comparison). We subsequently consider the full measured times series from buoy 41036.

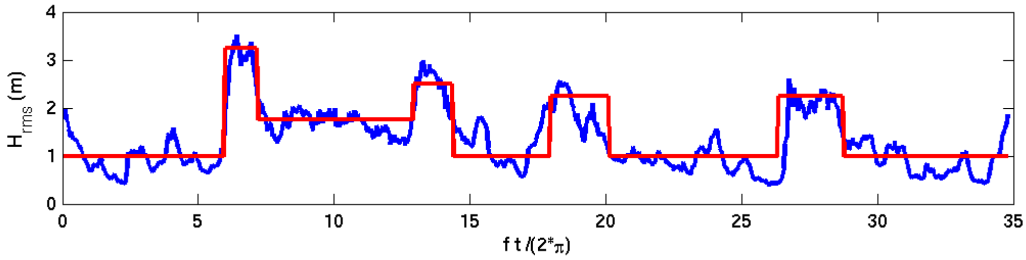

Figure 1: Time series of wave height (recorded hourly) at NDBC buoy 41036 during March 2013. Shown are the actual measured wave height time series (blue) and the approximate time series (red). Note that the abscissa contains a normalized time axis, where the normalization is carried out with the Coriolis parameter f for mid-latitudes.

3.1. *Steady state solution*

First, results for the intermediate wave height case (H=2.25m) are discussed. The variation of the cross-shore (*U*) and alongshore (*V*) currents with cross-shore position and depth are shown in Figure 2. In this case, the surf zone is approximately 300m wide, and an offshore-directed undertow current is evident. An analysis of the momentum balances (not shown) confirms that this undertow current is primarily driven by the body force associated with the wave forcing terms and is also affected by the surface shear stress due to the presence of the rollers as well as bottom boundary layer processes. As expected, the Coriolis term in the momentum equation or the Coriolis-Stokes term are not large enough to cause any modification to the flow in the surf zone. These findings are in agreement with other previous studies and have also been discussed in Özkan-Haller (2013). Further, no alongshore current component exists in the surf zone, consistent with the usual surf zone balance for normally incident waves.

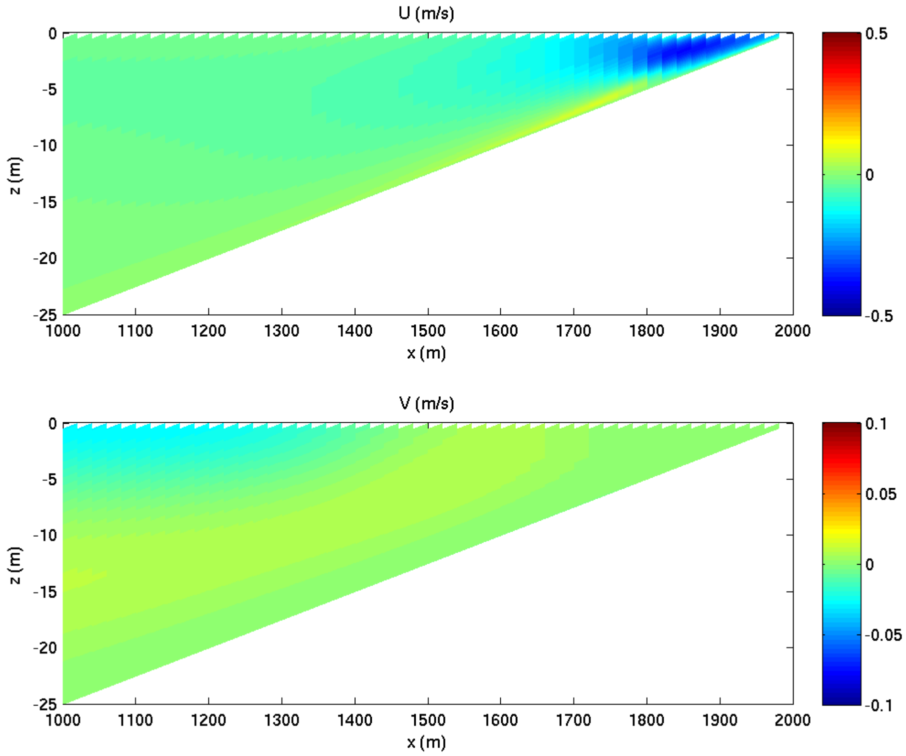

Figure 2: Steady-state cross-shore (top panel) and alongshore (bottom panel) currents for waves of 2.25m wave height

Figure 2 further suggests that, once outside the surf zone, a weak offshore-directed current still exists (returning the shoreward volume flux due to the Stokes drift), and this current becomes surface-intensified as distance from shore increases. This is also consistent with previous theoretical and observational studies (see, for example, Lentz and Fewings, 2012). In this region a weak alongshore directed jet is also created (also see Özkan-Haller, 2013). These features are affected by the Coriolis-Stokes stress which is primarily responsible for the depth-variations in the offshore directed undertow current in deeper water (h>20m or so). In the intermediate water depths, the Coriolis term in the momentum equations is also active, resulting in the alongshore-directed weak jet. This can essentially be interpreted as the undertow current being diverted alongshore as it exists out of the surf zone.

A few cross-shore positions are chosen (*x*=1580, 1660, 1820, and 1940m corresponding to water depth *h*=10.5, 8.5, 4.5, and 1.5m). Vertical profiles of cross-shore and alongshore currents are shown at these locations in Figure 3. The first two position are location in the shoaling region where the wave height is still increasing, the third position is located inside the surf zone. The cross-shore profiles show indication of boundary layer streaming near the bottom boundary and offshore-directed velocities further up in the water column. A weak surface-intensified alongshore current jet also exists.

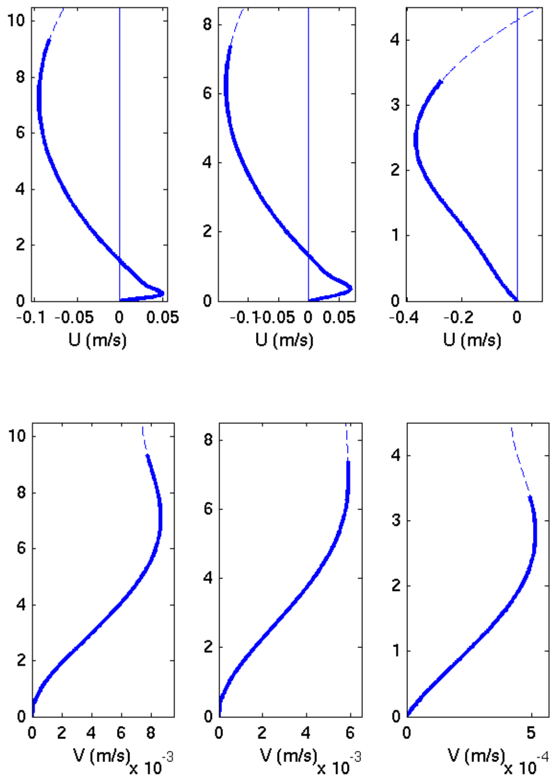

Figure 3: Vertical profile of cross-shore velocities (top panels) and alongshore velocities at cross-shore positions (from left to right) *x*=1580, 1660, and 1820m, corresponding to water depths of 10.5, 8.5, and 4.5m. Solid lines indicate the part of the water column below wave trough level.

Note that at this intermediate water depth the resulting velocities are small (5-10 cm/s) but comparable to wind-induced flows at these depths. All forcing mechanisms are generally weak, but almost all forcing terms contribute to the final flow profile. Note also that an alongshore current component is generated outside the surf zone despite normal wave incidence, balancing part of the body force due to wave and setup gradient effects through the Coriolis term (so that shoreward-directed forcing results in an alongshore flow). The cases involving smaller (1m) and larger (3.25m) wave heights result in qualitatively similar results, although the surf zone width and current magnitudes vary quantitatively.

3.2. *Time-dependent solution for steady wave forcing*

Next, we analyze cases involving the same wave conditions considered in section 3.1; however, the time-dependent result is of interest now. Note that the wave forcing is steady, but the flow is allowed to begin from rest and ramp up to the steady solution discussed above. Near-surface currents are analyzed at the chosen cross-shore positions (*x*=1580, 1660, 1820, and 1940m corresponding to water depth *h*=10.5, 8.5, 4.5, and 1.5m). Figure 4 shows the time series at *x*=1660m (*h*=8.5m) for the case involving waves of 1m height. The time axis is normalized using the Coriolis parameter for mid-latitudes; hence a normalized value of unity corresponds to approximately 20hours.

Evident in Figure 4 are inertial oscillations that decay over the course of several days, and the flow eventually converged to the steady state conditions discussed above. The decay time scale is a function of the ratio of the local eddy viscosity to the Coriolis parameter. Since the eddy viscosity increases rapidly as one approaches the surf zone from offshore, the decay time scale shortens rapidly towards the surf zone as well. At a point a few hundred meters shoreward (at x=1820m, h=4.5m), the steady state solution is reached within a few hours, and no inertial oscillations are obtained.

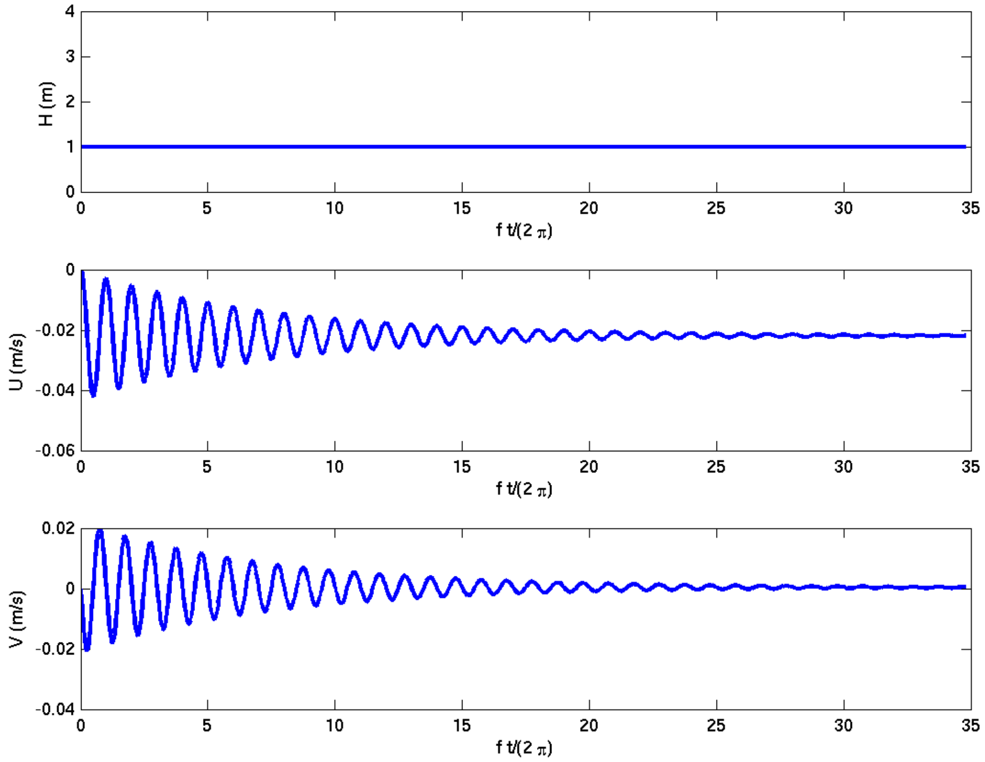

Figure 4: Temporal variability of wave height (top), and near-surface cross-shore current (middle) and alongshore current (bottom) at x=1660m. The case involves wave height of 1m.

For the case involving waves with height 2.25m, the eddy viscosity is generally larger in the entire domain, and the transition to the steady solution at x=1660m (h=8.5m) occurs with quickly with no time for inertial oscillations. Further offshore, at x=1580m (h=10.5m), only a few inertial oscillations are predicted before the steady state solution is reached (see Figure 5). Note that both of these positions are in the shoaling zone where the wave height continues to increase, although some wave dissipation already exists. Finally, for the case involving 3.5m waves, the eddy viscosity everywhere in the domain is large enough (>0.025 m^2/s) that the steady state solution is reached quickly everywhere.

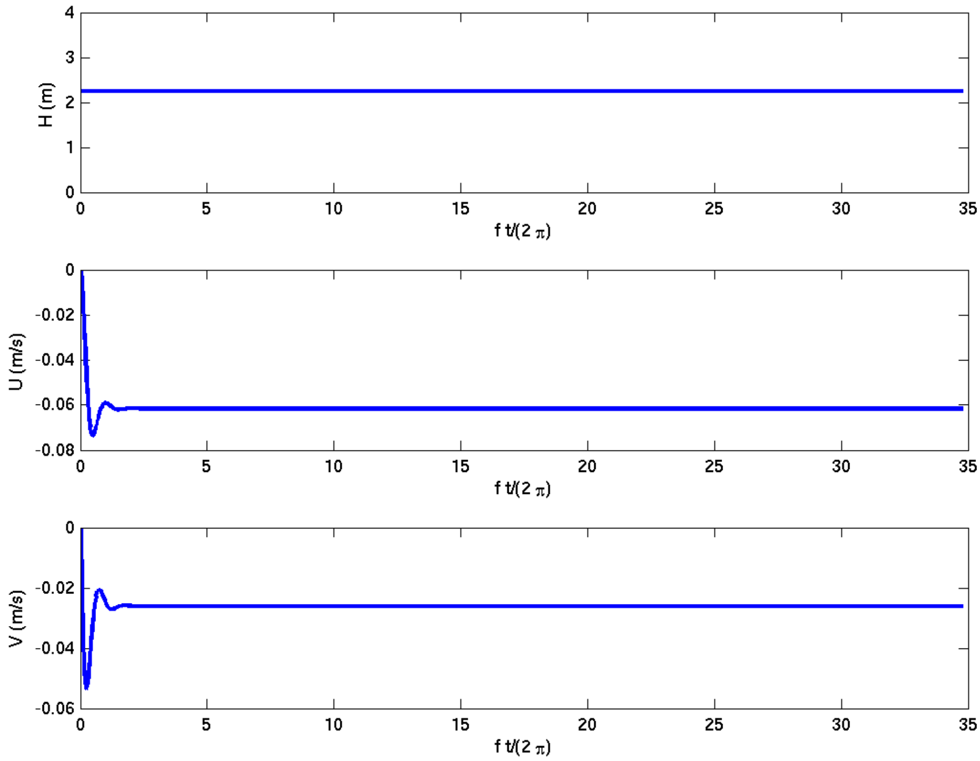

Figure 5: Temporal variability of wave height (top), and near-surface cross-shore current (middle) and alongshore current (bottom) at *x*=1660m. The case involves wave height of 2.25m.

3.3. *Time-dependent solution for abruptly-varying wave forcing*

The results in the previous section suggest that the transition to the steady solution happens quickly in and near the surf zone. However, just outside the surf zone a few inertial oscillations may be present. Far away from the surf zone in water depths of O(10m) where the magnitude of the eddy viscocity is at least an order of magnitude smaller than in the surf zone, several inertial oscillations are predicted before the steady state solution is reached. We now take the next step and investigate the effect of any inertial oscillations in a setting where the offshore wave height changes in time (over time scales that are larger than the inertial time scale). We first construct a piece-wise smooth time series of wave heights (see Figure 1) that mimics the observed time series at NDBC buoy 41036. Our objective is to observe the sequential transition to the steady solutions associated with each successive wave condition.

This expected behavior is indeed predicted outside the surf zone at *x*=1660m (*h*=8.5m), see Figure 6. Note that during periods of time with larger incident wave action, this cross-shore position is located just outside the surf zone (and hence experiences larger eddy viscosities and faster convergence to the steady state response) compared to times when waves are smaller and the eddy viscosity is markedly smaller.

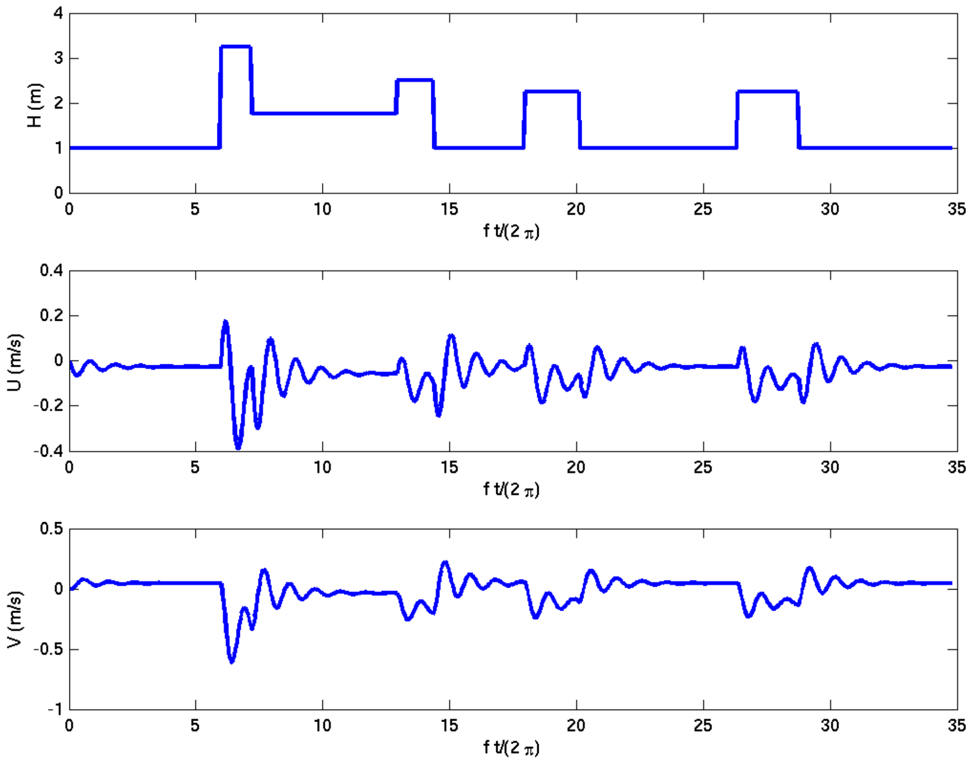

Figure 6: Temporal variability of wave height (top), and near-surface cross-shore current (middle) and alongshore current (bottom) at *x*=1660m. The case involves a sequence of consecutive wave events mimicking the observed data set.

3.4. ***Time-varying solution for a realistic wave time series***

Finally, we construct a solution for the case involving the observed time series at NDBC buoy 41036. The results (Figure 7) indicate that the behavior at *x*=1660m (*h*=8.5m) is consistent with the case involving an idealized sequence of wave events. In particular, the resulting circulation appears to be highly correlated with the wave signal at times when the waves are relatively large. For example, during the large storm with wave heights of 3.5m, the response in the cross-shore undertow currents is timed to correspond to the arrival of the large waves. This can be explained by the fact that this cross-shore position is located closer to the surf zone during high wave events, hence the eddy viscosity value at this location is larger during those times.

The situation appears to be different during periods of lower wave action. During these times, the resulting circulation can be markedly different from the steady state response, at times resulting in stronger currents than those predicted by a steady state model. This is especially so for the predicted alongshore currents. Also, the resulting velocity peaks during low wave regimes are not necessarily timed to arrive simultaneously as the waves, primarily because the circulation system is still responding to an earlier (larger) wave event.

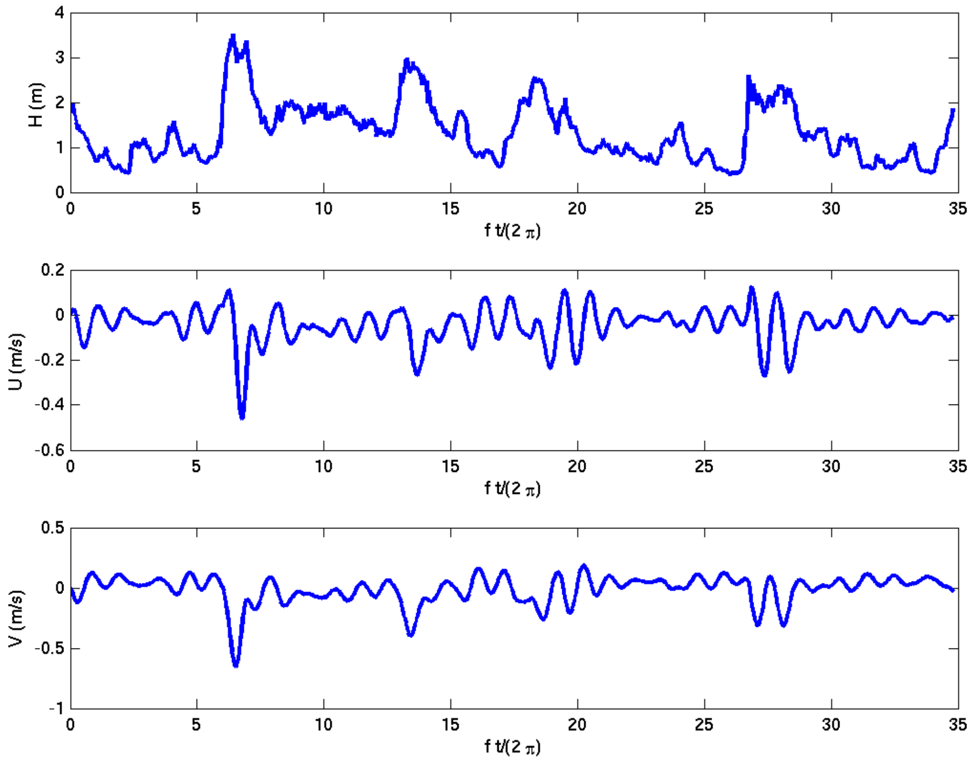

Figure 7: Temporal variability of wave height (top), and near-surface cross-shore current (middle) and alongshore current (bottom) at *x*=1660m. Wave height time series corresponds to the observed waves at NDBC buoy 41036 during March 2013.

Finally, Figure 8 depicts the temporal response a few hundreds of meters shoreward at *x*=1820m. During the larger wave event this location experiences some wave breaking. Therefore, eddy viscocity values are larger at this location and response times are shorter.

4. Summary

Effects related to Earth's rotation are generally neglected in models of nearshore circulation. However, results reported here using a canonical example case involving a plane beach and waves characteristic of the East Coast of the US suggest that the effects of Earth's rotation may be significant just outside the surf zone. Further, considerations of the time-dependent nature of the response (potentially involving oscillations at the inertial time scale) point at situations where the transient response could result in currents that are stronger than suggested by the steady state solution. Also, in these cases the circulation response can lag behind the arrival of a wave event. Undoubtedly, further work is required to sort out strong sensitivities to eddy viscosity values and determine the applicability (and observability) of the circulation features suggested by these results.

Acknowledgements

We acknowledge funding from Oregon Sea Grant and the National Science Foundation.

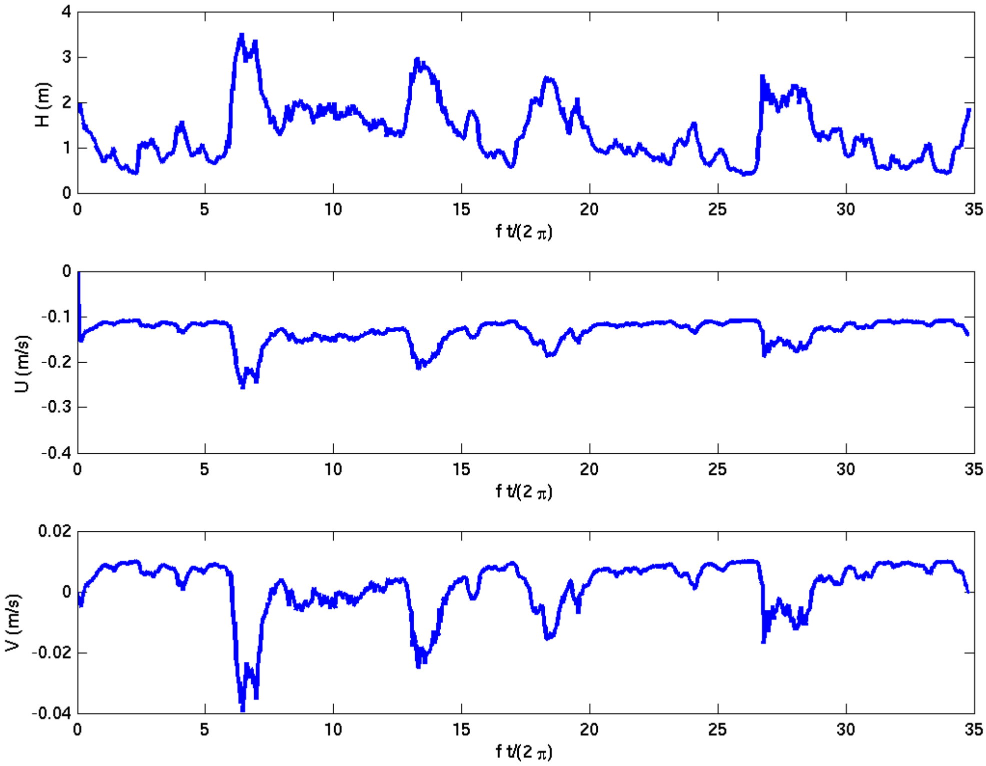
H (m)
f t/(2 π)
U (m/s)
f t/(2 π)
V (m/s)
f t/(2 π)

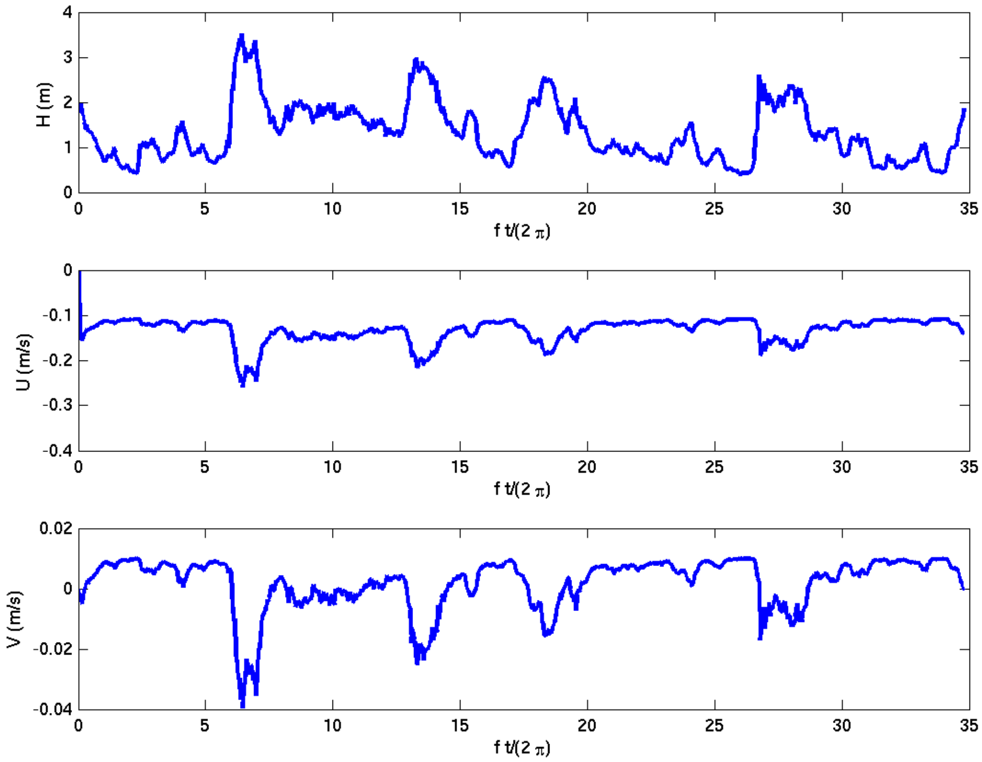
H (m)
f t/(2 π)
U (m/s)
f t/(2 π)
V (m/s)
f t/(2 π)